

## Sequential population of adsorption sites driven by surface stress

D. Sander,<sup>1,\*</sup> H. L. Meyerheim,<sup>1</sup> Z. Tian,<sup>1</sup> L. Niebergall,<sup>1</sup> N. N. Negulyaev,<sup>2</sup> K. Mohseni,<sup>1</sup> V. S. Stepanyuk,<sup>1</sup> R. Felici,<sup>3</sup> and J. Kirschner<sup>1</sup>

<sup>1</sup>Max-Planck-Institut für Mikrostrukturphysik, Weinberg 2, D-06120 Halle, Germany

<sup>2</sup>Fachbereich Physik, Martin-Luther Universität, Halle-Wittenberg, Friedemann-Bach-Platz 6, D-06099 Halle, Germany

<sup>3</sup>ESRF, ID-03, BP 220, F-38043 Grenoble, France

(Received 22 February 2010; published 8 April 2010)

We performed a combined experimental and theoretical study of surface stress and structure of the adsorption of oxygen on Ir(001). We find that up to an oxygen coverage of half a monolayer oxygen adsorbs in bridge sites, whereas at larger coverage between 0.5 and 0.75 adsorption occurs in both bridge and hollow sites. A compressive surface stress change of  $-2.2$  N/m is measured, and substantial lattice relaxations are identified by surface x-ray diffraction. Density-functional theory calculations reveal that anisotropic O-induced surface stress is a key factor for the sequential occupation of the adsorption sites.

DOI: [10.1103/PhysRevB.81.153403](https://doi.org/10.1103/PhysRevB.81.153403)

PACS number(s): 61.05.cf, 68.35.B-, 68.43.-h, 68.49.-h

Adsorption processes induce modifications of the geometric structure and the physical properties of the substrate surface. Examples include adsorbate-induced surface reconstructions<sup>1</sup> and modified magnetic properties.<sup>2</sup> The extent of the adsorbate-induced modification of substrate properties decisively depends on the adsorption site. Understanding the mechanisms which drive the adsorption of an atomic species on a certain adsorption site is therefore of high interest in many branches of surface science.

In an attempt to classify adsorption sites, it has been argued—based on effective medium theory—that a highly coordinated adsorption site should be energetically favorable in general. Thus, the common belief emerged that on low index surfaces such as the (001) surface of face centered cubic (fcc) metals, highly coordinated adsorption sites are occupied. But, it has been shown that in some cases exceptions from the rule exist. An *a priori* prediction of a specific adsorption site remains illusive at present. In this context the adsorption of oxygen on Ir(001) represents an archetype model, where low-energy-electron-diffraction (LEED) experiments in combination with density-functional theory (DFT) calculations have shown that oxygen atoms occupy the “unusual” bridge site.<sup>4</sup> This is an unusual adsorption site as it is characterized by a reduced coordination (twofold) as compared to the fourfold coordination of a hollow site.

To investigate the driving force for the population of the unusual bridge site adsorption we have applied an unique combination of surface stress and surface x-ray diffraction (SXRD) measurements during the formation of the oxygen adsorbate structure on Ir(001). Our experiments are complemented by DFT calculations of the energetics, atomic structure, and surface stress of this system. Surface stress contributes to the Helmholtz free energy of the surface.<sup>3</sup> Our measurements of adsorbate-induced surface stress *changes* reveal the strain dependence of the surface tension,<sup>3</sup> which is compared to the results of the DFT calculations.

Previous work has suggested that bridge site adsorption is favored due to attractive interactions between oxygen atoms. This contrasts with hollow site adsorption, where repulsive interactions have been predicted.<sup>4</sup> Our results question this qualitative assessment.

Our study reveals significant compressive surface stress

changes upon O-adsorption, in connection with sizeable structural distortions at the surface. These findings mark a major progress for the understanding of the physical principles which govern the selection of adsorption sites by identifying anisotropic stress and strain relaxation as important aspects of the adsorption process.

The SXRD experiments were carried out at the beamline ID03 of the European Synchrotron Radiation Facility (ESRF) in Grenoble (France).<sup>5</sup> The surface stress measurements were performed in a separate UHV chamber also equipped with a LEED setup.

For both measurements, we prepared a clean Ir(001)-(1 × 1) surface as described earlier.<sup>6</sup> The preparation includes repeated cycles of ion bombardment (Ar<sup>+</sup>, 1.5 keV, 3 μA), annealing (1500 K) under UHV conditions, annealing (1300 K) and cool down to 300 K in an oxygen partial pressure of  $p_{\text{O}_2} = 2 \times 10^{-6}$  mbar. Finally, heating in hydrogen ( $p_{\text{H}_2} = 2 \times 10^{-7}$  mbar) at 530 K removes oxygen. This leads to a clean Ir(001)-(1 × 1) surface, as checked by SXRD, LEED, and Auger electron spectroscopy. The O-adsorbate structure was prepared by exposing the Ir(001)-(1 × 1) substrate to oxygen at  $p_{\text{O}_2} = 1.2 \times 10^{-6}$  mbar at 550 K.

To compensate for the x-ray induced desorption of oxygen from the surface, we offered a continuous supply of atomic oxygen by keeping a constant oxygen partial pressure of  $1.2 \times 10^{-6}$  mbar in the presence of a glowing tungsten filament. This procedure leads to a steady-state oxygen coverage of  $\theta \approx 0.7$  ( $\theta = 1 : 1.36 \times 10^{15}$  atoms/cm<sup>2</sup>) for both experiments as verified by SXRD.

We measured the oxygen-induced surface stress change by monitoring the curvature change upon oxygen exposure of a 0.1-mm-thin Ir substrate (length: 12 mm, width: 2.5 mm) with an optical deflection technique, described in detail earlier.<sup>7</sup> The result presented in Fig. 1 reveals that upon oxygen exposure at  $1.2 \times 10^{-6}$  mbar at 550 K a compressive surface stress change of  $-2.2$  N/m is measured, which saturates already after 20 s. The ongoing exposure to oxygen at 550 K does not change the stress further. This surface stress change is ascribed to the formation of the oxygen adsorbate structure on Ir(001) with an O-coverage of 0.7 as deduced from the quantitative SXRD analysis presented below. A

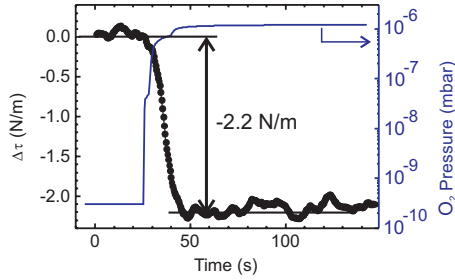


FIG. 1. (Color) Measured surface stress change in Ir(001)  $\Delta\tau$  (left scale) during oxygen exposure at  $1.2 \times 10^{-6}$  mbar (left scale) at 550 K. 20 s after the leak valve has been opened, a compressive surface stress change of  $-2.2$  N/m is measured, which does not change further during the ongoing  $O_2$  exposure. As discussed in the text this stress change is ascribed to an oxygen coverage of 0.7.

qualitative inspection of the sharp LEED pattern identifies two  $1 \times 2$  domains rotated by  $90^\circ$ .

To resolve the resulting surface structure and to determine the oxygen coverage, we performed SXRD measurements ( $\lambda = 0.62 \text{ \AA}$ ) on an identically prepared sample. We obtain structure factors  $|F_{obs}|$ , which were derived from integrated intensities from the SXRD analysis after correcting for geometric factors.<sup>8,9</sup> The standard deviation of  $|F_{obs}|$  is 7% on average. It is given by the counting statistics and by the deviation of intensities of symmetry equivalent reflections. In Figs. 2(a)–2(e) solid symbols represent the observed structure factor amplitudes ( $|F_{obs}|$ ) along five superlattice rods, which were measured up to a maximum momentum transfer of  $L = q_z/c^*$  of 3.25 reciprocal lattice units, where  $c^* = (1/3.84) \text{ \AA}^{-1}$  represents one reciprocal lattice unit.

Lines through the data points of Figs. 2(a)–2(e) represent

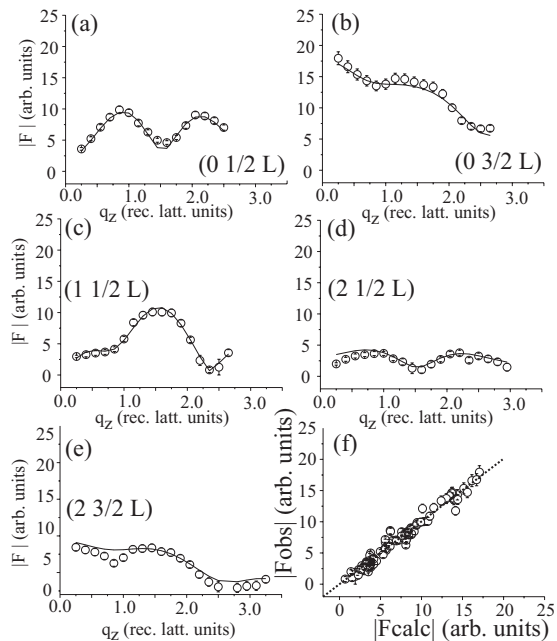


FIG. 2. [(a)–(e)] Measured (symbols) and calculated (lines) structure factor amplitudes along five superlattice rods. (f) Plot of observed (obs) versus calculated (calc.) structure factor amplitudes for all 99 reflections.

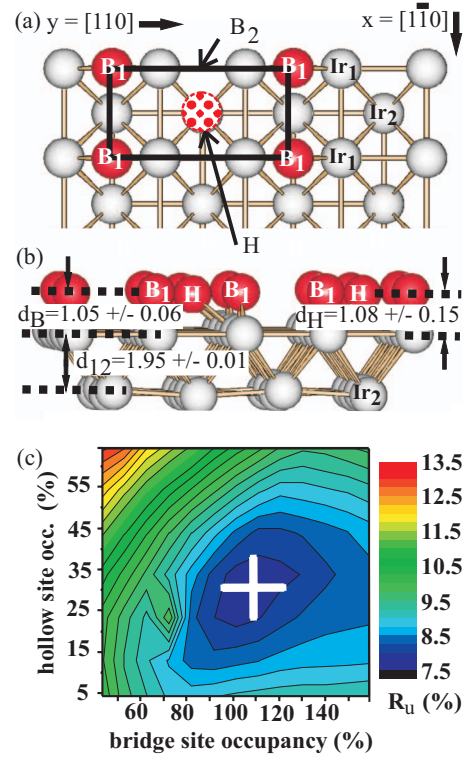


FIG. 3. (Color) (a) Structure model for  $O/Ir(001)-(2 \times 1)$  in top view. The rectangle shows a  $1 \times 2$  unit cell, the arrows  $H$  and  $B_2$  indicate adsorption for  $\theta > 0.5$  in hollow (red dotted sphere) and hypothetical bridge sites (see also Fig. 4), respectively. The side view (b) along the  $y$  direction identifies bridge ( $B_1$ ) and  $H$  sites, assuming full hollow site occupation for clarity. Surface and subsurface Ir atoms are labeled  $Ir_1$  and  $Ir_2$ , respectively. The Ir layer spacing is given by  $d_{12}$ . Distances in  $\text{\AA}$ . (c) Contour plot of the fit quality as given by the unweighted residuum  $R_u$  of the model shown in (a) and (b). The white cross marks the best fit quality at full population of 100% of bridge sites ( $B_1$ ) and additional adsorption of 30% in hollow sites.

the best fit, using the structure model discussed below. The quality of the fit is characterized by the unweighted residuum ( $R_u$ ) or the goodness of fit (GOF).<sup>10,11</sup> Excellent values of  $R_u = 0.075$  and  $GOF = 0.9$  are achieved. This excellent quality of the fit is also apparent in Fig. 2(f). Here, both  $|F_{obs}|$  and  $|F_{calc}|$  of the same  $(hkl)$  are plotted for all data, including 15 in-plane  $(hk0)$  reflections. The diagonal line represents the best condition  $|F_{obs}| = |F_{calc}|$ . This condition is fulfilled to an excellent degree, and deviations are generally smaller than the  $1\sigma$  standard deviation.

The structural model derived from the least-squares fitting is presented in Fig. 3(a) in top view. Oxygen atoms (red) are located in bridge sites ( $B_1$ ) next to the surface layer Ir atoms (gray,  $Ir_1$ ), and in hollow ( $H$ ) sites. O-adsorption in subsurface sites is ruled out due to the resulting significantly inferior fit quality. The most remarkable result of the analysis is the partial occupancy of  $H$  sites in addition to fully occupied bridge sites ( $B_1$ ).

The occupation of bridge and hollow site has not been reported before, and it comes as a surprise. Therefore we check the significance of this result by plotting the quality of

the structural model, as given by  $R_u$ , for a variation in the population of both bridge sites ( $B_1$ ) and  $H$  sites in Fig. 3(c). In varying the respective populations, all other parameters ( $z$  coordinates for oxygen and two Ir-atoms, one  $y$  coordinate for Ir, and three different Debye parameters representing disorder) were simultaneously allowed to vary, i.e., parameter correlations are included. The location of the minimum of the contour plot of Fig. 3(c) clearly reveals that the best structural model is obtained for an occupancy of  $110 \pm 25\%$  for the bridge site and of  $30 \pm 15\%$  for the hollow site. This model determines the oxygen coverage as  $\approx 0.70 \pm 0.15$ . An occupancy of 100% marks the upper limit, and we conclude that a completely occupied bridge site is a characteristic of this structure.

Important structure parameters are derived with high accuracy from this model, which shed light onto the adsorption geometry. (i) We find vertical adsorption heights of  $d_H = 1.08 \pm 0.15$  and  $d_B = 1.05 \pm 0.06$  Å for the  $H$  and  $B_1$  site above the first Ir layer. This corresponds to interatomic Ir-O distances of  $2.17 \pm 0.10$  and  $1.76 \pm 0.10$  Å for the  $H$  and  $B_1$  sites, respectively. These values are within the reported range of Ir-O compounds.<sup>12</sup> The adsorption heights are about 0.2 Å less than previously reported in a LEED study ( $d_B = 1.30 \pm 0.04$  Å), where only bridge sites were considered.<sup>4</sup> We may ascribe this to a larger O-coverage in our case, and lowering the adsorption height might be a measure to reduce the repulsive Coulomb interaction between oxygen atoms by “digging” into the Ir-surface. (ii) The first Ir-atoms ( $Ir_1$ ) are shifted laterally by  $\delta = 0.052 \pm 0.005$  Å (Ref. 4:  $0.075 \pm 0.030$  Å) out of their bulk truncated positions, while there is a small rumpling of  $\Delta Ir_2 = 0.04 \pm 0.01$  Å within the second Ir-layer (Ref. 4:  $0.038 \pm 0.034$  Å). These minute displacements are not visible in the structural model of Figs. 3(a) and 3(b), but they suggest that row-pairing, i.e., a small lateral relaxation of Ir atoms underneath the oxygen atoms of bridge sites, persists even for the partial occupation of hollow sites.

We carried out total energy DFT calculations to provide a deeper understanding of the underlying principles which stabilize the unusual surface geometry and the resulting compressive surface stress change. The calculations were performed within the generalized-gradient approximation using the exchange-correlation potential developed by Perdew, Burke, and Ernzerhof.<sup>13</sup> We employed the SIESTA (Ref. 14) code with its localized atomic orbital basis sets and pseudopotential representation of the core states. The pseudopotentials were generated according to the procedure of Troullier and Martins.<sup>15</sup> We used a double- $\zeta$  plus polarization (DZP) orbital for describing the valence electrons. An energy cutoff of 300 Ry was set to define the real-space grid for numerical calculations involving the electron density. For fcc Ir bulk we found an equilibrium lattice constant  $a = 3.905$  Å. The optimized unit cell was used as the basis to construct all slabs for the surface calculations. The Ir(001) surface was modeled using five-layer slabs, with three bottom layers kept fixed. To describe the (001) surface and the adsorption of oxygen atoms we have used  $4 \times 4$  supercells.

Our calculations indicate adsorption in bridge sites for an oxygen coverage of  $\theta = 0.5$ . A  $1 \times 2$  superstructure is formed, where O-adatoms do not share the same Ir atom. This result

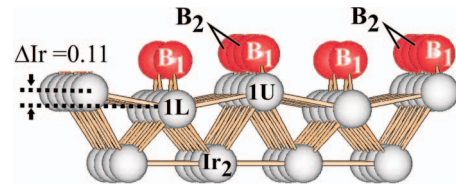


FIG. 4. (Color) Model based on calculations only of the hypothetical adsorption in both bridge sites ( $B_1$  and  $B_2$ ) at a total coverage of 0.75. View as in Fig. 3(b). Note the pronounced rumpling of the topmost Ir layer of  $\Delta Ir = 0.11$  Å, which is absent in the structure model presented in Fig. 3(b).

agrees with the previous experimental and theoretical study.<sup>4</sup>

We offer insight into the adsorption process by studying how the selection of an adsorption site depends on coverage. Our calculations reveal an unexpected change in adsorption site with increasing O-coverage  $\theta$  above 0.5, which goes beyond common wisdom, and which has not been described before. For  $\theta = 0.56$  (one extra O-adatom in the  $4 \times 4$  supercell), an extra O-adatom prefers to occupy another bridge site [ $B_2$  in Fig. 3(a)] rather than the hollow site [ $H$  in Fig. 3(a)]. The energy difference between these atomic configurations is 0.10 eV/extra atom. Surprisingly, further increasing the O-coverage induces a reversal of the stability of adsorption sites. For  $\theta = 0.75$ , two adsorption sites ( $H$  and  $B_2$ ) are considered, as shown in Figs. 3(a). The energy gain for adsorption in the hollow sites is about 0.145 eV/extra O-adatom (0.58 eV/cell) as compared to adsorption in bridge sites. Thus, additional adsorption in hollow sites is favored in this coverage regime.

Increasing the O-coverage above 0.75, again a reversed stability of adsorption sites is deduced from the changes of total energy. Two adsorbate structures corresponding to  $\theta = 1.0$  are considered. In the first case, 0.5 ML of O is adsorbed in bridge sites ( $B_1$ ), and an additional 0.5 ML of O is adsorbed in  $H$  sites. This atomic structure is energetically less favorable than the second one, where the full oxygen coverage of  $\theta = 1$  is adsorbed in bridge sites ( $B_1$  and  $B_2$ ). The total energy of the latter is lower by 0.73 eV/extra O adatom, as compared to adsorption in bridge and hollow sites. Since a coverage  $\theta \geq 0.75$  is not accessible under the applied experimental conditions, we focus on the coverage regime 0.5–0.75 in the following.

Our calculations suggest stress and strain relief in the topmost Ir(001) layers as the driving force behind the reversal of stability of adsorption sites for  $0.56 < \theta < 0.75$ . Recent studies have demonstrated that this mechanism could substantially affect growth phenomena on surfaces.<sup>16,17</sup> Here, oxygen-adsorption at  $\theta = 0.75$  does not occur in bridge sites. This would increase the stress of the system. The adsorbate-substrate system reacts with sizeable local distortions. As a result, the O adsorption in bridge sites ( $B_1, B_2$ ) induces a strong corrugation of the topmost Ir layer (atoms 1L, 1U) of 0.11 Å, as indicated in Fig. 4. This configuration has a larger total energy, as compared to that shown in Figs. 3(a) and 3(b), and consequently it is not observed experimentally.

Both experiment and theory identify a compressive surface stress change upon O adsorption. We measure a surface stress change of  $-2.2$  N/m. This value compares favorably

with the calculated average surface stress change with respect to the clean Ir surface of  $-2.8$  N/m. These numbers reveal that the tensile surface stress of clean Ir changes in the compressive direction upon O adsorption. Whereas the surface stress of clean Ir(001) is calculated at  $+4.0$  N/m, O adsorption lowers this tensile stress significantly and in an anisotropic manner, which depends on O coverage. We calculate a surface stress of  $+0.3$  N/m along the  $x$ -axis in Fig. 3, and  $+2.1$  N/m in the perpendicular direction ( $y$  axis in Fig. 3) for adsorption at a coverage of 0.5 in bridge sites ( $B_1$ ) only. At a larger coverage of 0.75 with the site population as depicted in Fig. 3(a) we derive  $+0.8$  and  $+1.6$  N/m for the former and the latter direction, respectively. The reduction in tensile stress is strongest along the direction of adjacent O adsorbates along the  $x$  axis of Fig. 3 and much smaller in the perpendicular direction. Population of hollow sites reduces this surface stress anisotropy. The *average* surface stress is the same at both coverages, and it amounts to  $+1.2$  N/m. Thus, the additional population of hollow sites is an isosurface stress process. This is most remarkable, as adsorbate-induced surface stress changes have been reported to grow monotonous with adsorbate coverage,<sup>7</sup> which is not the case here.

The calculations reveal that the *absolute* magnitude of

O-induced surface stress remains positive, but its magnitude is considerably larger for the clean Ir(001) surface as compared to the O-covered surface. Therefore, the previous notion that an attractive O-O interaction could stabilize the “unusual” bridge site of the  $1 \times 2$ -O structure appears questionable. An attractive interaction should lead to a larger tensile surface stress, which is not observed. Our results rather suggest that O adsorption leads to repulsive and anisotropic interactions within the surface layer. The O-induced anisotropy of surface stress has been neglected in previous work,<sup>4</sup> but it appears to be a critical point of the proper assessment of adsorbate interactions.

In conclusion, our study reveals that simple coordination arguments might be misleading for the prediction of specific adsorption sites. Our combined experimental and theoretical work rather identifies a subtle interplay among adsorption, structural relaxation, and surface stress. Only the quantitative analysis of all these aspects allows for a reliable characterization of the driving force for the sequential population of different adsorption sites with increasing coverage.

We thank the ESRF staff for hospitality and support. This work was supported by the DFG through SFB 762.

\*sander@mpi-halle.mpg.de

<sup>1</sup>H. Ibach, *Surf. Sci. Rep.* **29**, 195 (1997); **35**, 71 (1999) and references therein.

<sup>2</sup>D. Sander, W. Pan, S. Ouazi, J. Kirschner, W. Meyer, M. Krause, S. Müller, L. Hammer, and K. Heinz, *Phys. Rev. Lett.* **93**, 247203 (2004).

<sup>3</sup>H. Ibach, *Surf. Sci.* **603**, 2352 (2009).

<sup>4</sup>K. Johnson, Q. Ge, S. Titmuss, and D. A. King, *J. Chem. Phys.* **112**, 10460 (2000).

<sup>5</sup>S. Ferrer and F. Comin, *Rev. Sci. Instrum.* **66**, 1674 (1995).

<sup>6</sup>K. Heinz, G. Schmidt, L. Hammer, and K. Müller, *Phys. Rev. B* **32**, 6214 (1985).

<sup>7</sup>D. Sander, Z. Tian, and J. Kirschner, *J. Phys.: Condens. Matter* **21**, 134015 (2009).

<sup>8</sup>C. Schamper, H. L. Meyerheim, and W. Moritz, *J. Appl. Crystallogr.* **26**, 687 (1993).

<sup>9</sup>E. Vlieg, *J. Appl. Crystallogr.* **30**, 532 (1997).

<sup>10</sup> $R_u$  is defined as  $R_u = \frac{\sum |F^{obs}| - |F^{calc}|}{\sum |F^{obs}|}$ , with  $F^{obs}$  and  $F^{calc}$  as observed and calculated structure factors, respectively. For GOF see Ref. 11.

<sup>11</sup>R. Feidenhans'l, *Surf. Sci. Rep.* **10**, 105 (1989).

<sup>12</sup>See, e.g., Inorganic Crystal Structure Data Base, <http://icsd.ill.edu/icsd/index.html>

<sup>13</sup>J. P. Perdew, K. Burke, and M. Ernzerhof, *Phys. Rev. Lett.* **77**, 3865 (1996).

<sup>14</sup>J. M. Soler, E. Artacho, J. D. Gale, A. Garcia, J. Junquera, P. Ordejón, and D. Sanchez-Portal, *J. Phys.: Condens. Matter* **14**, 2745 (2002).

<sup>15</sup>N. Troullier and J. L. Martins, *Phys. Rev. B* **43**, 1993 (1991).

<sup>16</sup>V. S. Stepanyuk, D. I. Bazhanov, A. N. Baranov, W. Hergert, P. H. Dederichs, and J. Kirschner, *Phys. Rev. B* **62**, 15398 (2000).

<sup>17</sup>X.-D. Ma, D. I. Bazhanov, O. Fruchart, F. Yildiz, T. Yokoyama, M. Przybylski, V. S. Stepanyuk, W. Hergert, and J. Kirschner, *Phys. Rev. Lett.* **102**, 205503 (2009).